

# Measurements of the tertiary rainbow

*(photo by Michael Großmann, taken at 2011-05-15)*

Dr. Alexander Haußmann  
Institut für Angewandte Photophysik

George-Bähr-Str. 1  
D-01069 Dresden  
+ 49 351 463 32858

[hausmann@iapp.de](mailto:hausmann@iapp.de)

## Image calibration and angular measurements

In order to prove that the color pattern in the photo is indeed the tertiary rainbow, a careful analysis of the angular distance from the sun was carried out by means of standard spherical geometry. From geometric optics, we expect the angles of extreme deviation for red (610 nm), green (530 nm) and blue (450 nm) to be  $41.6^\circ$ ,  $40.6^\circ$ , and  $39.1^\circ$  from the sun, respectively. The wavelengths were chosen to match approximately the sensitivity maxima of a typical CMOS sensor.

Since both position and time of the photograph are known, the calculation of the sun's position is easy and gives  $8.1^\circ$  elevation and  $289.6^\circ$  azimuth. The main task is to reconstruct these celestial coordinates for the individual pixels of the photograph as well. To do so, a star field image was taken with the same camera and the lens at the same zoom level. By this, it is possible to determine the relation between the field angle (angular distance of an object from the optical axis) and the pixel distance from the image center. In this particular case, we obtain (at the original image resolution):

$$R = 3633.7 \cdot \tan \vartheta - 262.45 \cdot \tan^2 \vartheta$$

Note that the first-order coefficient corresponds to a focal length of 18.9 mm, to be calculated from the sensor size of  $14.8 \times 22.2 \text{ mm}^2$  and the full image resolution of  $2848 \times 4272$  pixel. The second-order term represents a certain amount of Barrel distortion, as common for wide-angle zoom lenses.

Still left to determine are three angles which define the camera orientation. These are elevation and azimuth of the optical axis and the rotation of the sensor around this axis. The last parameter will be small, since usually the photographer will try to keep the horizon as a horizontal line in the image. Nonetheless, it cannot be neglected in order to achieve the necessary degree of accuracy in the analysis. All three angles can be calculated from only two reference points in the picture with known elevation and azimuth. Preferably, these will be stars or planets (as possible in NLC or moon halo photography). However, in our case, landmarks such as trees have to be chosen since they are the only long-term stable features in the picture.

The method of choice is therefore choosing two rather remote treetops or branches as references and calculate their unknown celestial coordinates from a star field picture taken as close as possible to the position of the tertiary bow photograph (Fig. 1). By this, parallax effects will be minimized. The three crucial angles for the star field image can be calculated easily from two stars. This indirect method gives as results for the tertiary bow image within an estimated error margin of  $0.2^\circ$ :

elevation of optical axis:	$18.7^\circ$
azimuth of optical axis:	$252.1^\circ$
image rotation:	$-2.6^\circ$ (image must be rotated clockwise to achieve a “horizontal horizon”)



*Fig. 1: Reference points for the determination of the image orientation. From the star field image (left), elevation and azimuth of the positions A and B can be calculated using stars as references. A and B can be identified in the original image taken from approximately the same position (right), thus serving as references to locate the recorded bow at the celestial sphere.*

Finally, it is now possible to calculate the angular distance of the points marked in Fig. 2 from the sun. Note that these were chosen to match the outer boundary of the red segment of the bow. This image is a processed and downsized version (285 x 428 pixel) of the original photo. The origin of the  $x$  and  $y$  pixel coordinates is the image center. The results are as follows:

x [pixel]	y [pixel]	elevation [°]	azimuth [°]	angular distance from sun [°]
17.5	121	37.3	256.5	41.8
10.5	109	35.6	255.1	41.8
4.5	99	34.1	253.8	41.9
-0.5	88	32.5	252.8	41.9
-4.5	75	30.6	251.9	41.8
-9.5	65	29.0	251.0	41.9
-12.5	53	27.1	250.3	41.7
-15.5	42	25.4	249.8	41.7
-18.5	31	23.7	249.2	41.7
-21.5	21	22.1	248.6	41.8
-23.5	10	20.4	248.2	41.8
-25.5	-3	18.3	247.9	41.8
-26.5	-14	16.6	247.7	41.8
-26.5	-24	15.0	247.6	41.7
-27.5	-35	13.3	247.4	41.8



*Fig. 2: Sample points (displayed white) at the outermost red rim of the recorded bow*

These data fit very well to the theoretical expectation of  $41,6^\circ$  distance from the sun. Explanations of the remaining differences may involve the actual sensor response spectrum (which is unknown in detail), drop-size dependent deviations from geometric optics, the finite diameter of the sun, or shifts of the bow position due to the strong image processing.

A second way to visualize the coincidence of the recorded bow with the theoretical tertiary rainbow position is to plot circles of equal angular distance from the sun in the correct

projection of the image (Fig. 3). By using the extreme deviation angles for RGB colors, it is possible to compare the bow with the prediction of geometric optics. As seen, the matching is very satisfying.

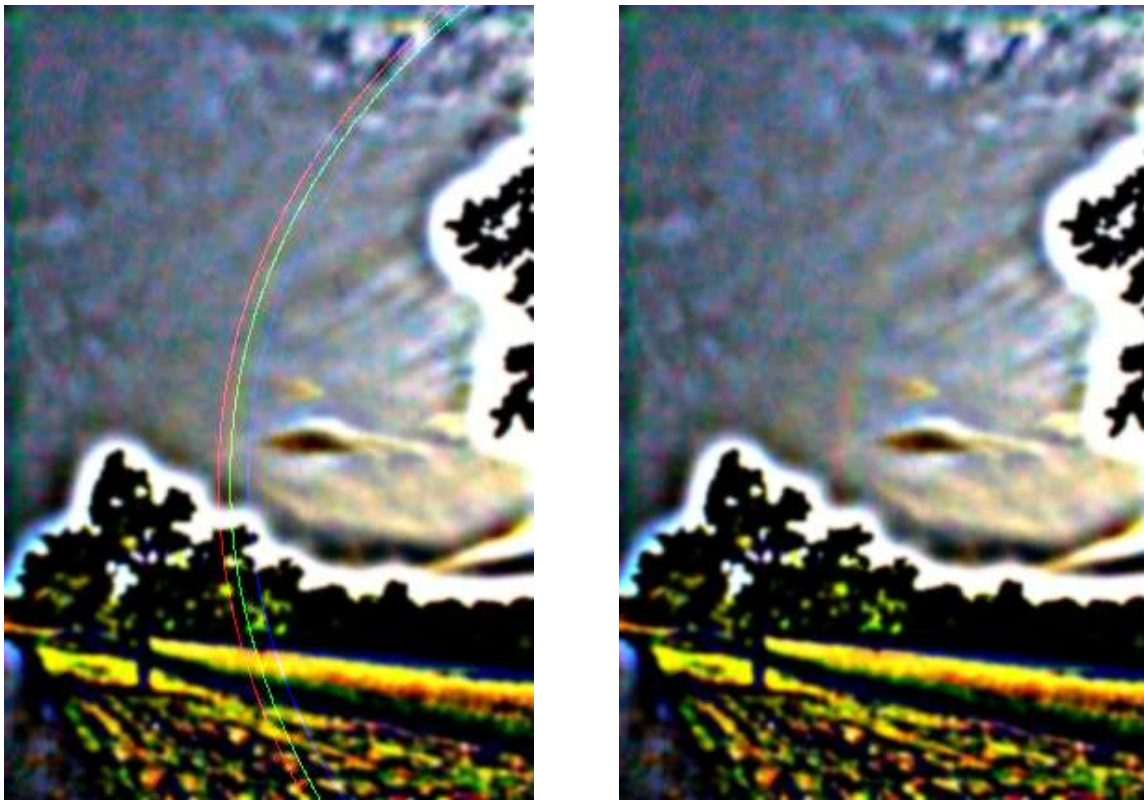


*Fig. 3: Left: Lines of equal angular distance from the sun:  $41,6^\circ$  (red),  $40,6^\circ$  (green),  $39,1^\circ$  (blue), corresponding to the extreme deviation angles for 610 nm, 530 nm and 450 nm. Right: Image without lines for comparison.*

### **Sector analysis**

Furthermore, a quantitative read-out of brightness data from the unprocessed image at original resolution was carried out. These data were averaged over  $40^\circ$  of solar-centered azimuth (sector angle) from  $29^\circ$  to  $59^\circ$  solar distance (Fig. 4). The results are shown in Fig. 5. As expected, the intensity steps of the bow are barely visible. This corresponds to the visual impression of the unprocessed image.

In order to extract the bow signal, a background subtraction was performed. The background characteristics for the individual channels were determined by fitting a polynomial of degree four to the regions apart from the bow. As a result, the bow signal is clearly visible in each channel, being shifted according to the dispersion between the individual colors. The extreme deviation angles for red, green and blue (vertical lines) match well the corresponding intensity maxima. The remaining small inward shift of each color maximum with respect to its extreme angle can be attributed to wave optics, being a familiar feature that can be treated with *Airy* theory. For other possible sources of error, see the previous section.

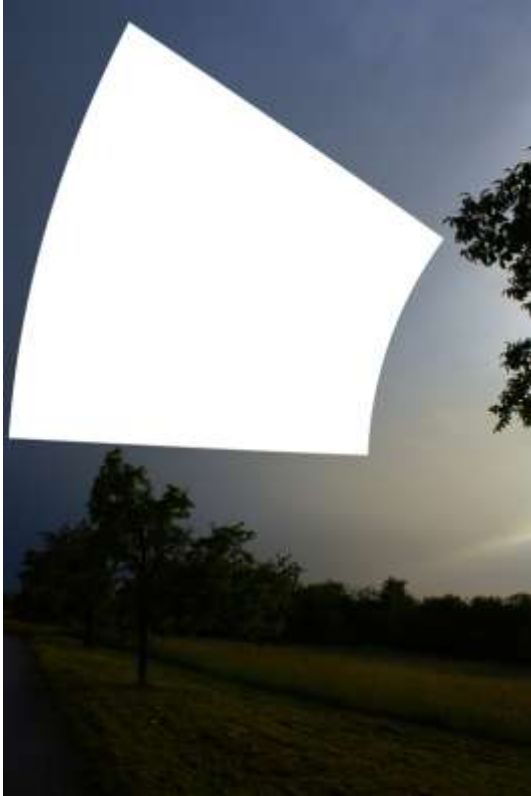


Fig. 4: Sector area (white) for quantitative analysis of intensity, covering solar distances from  $29^\circ$  to  $59^\circ$  along a  $40^\circ$  section of solar-centered azimuth.

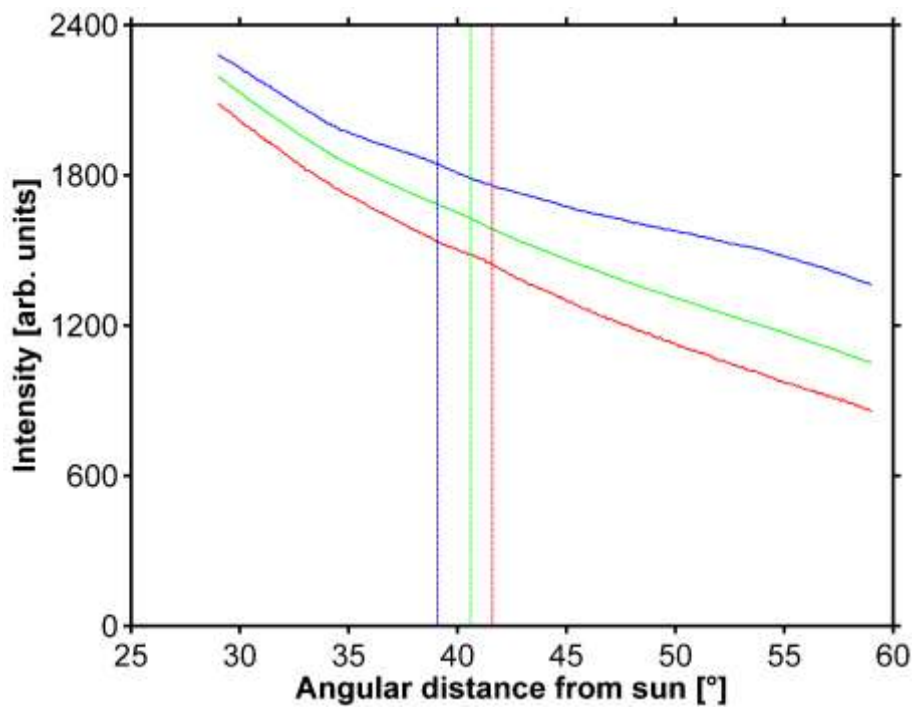
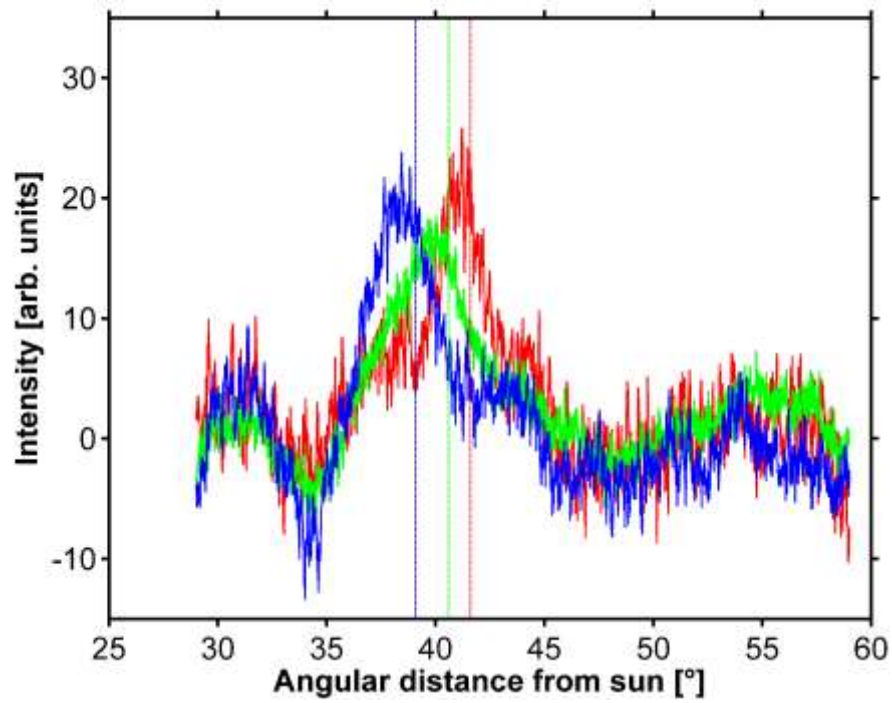


Fig. 5: Brightness data of the red, green and blue channel of the original image, averaged over a sector angle of  $40^\circ$ . The vertical lines mark the corresponding extreme deviation angles.



*Fig. 6: Background corrected brightness data. The maxima of the individual curves correspond to the recorded bow and match well the extreme deviation angles (vertical lines).*